Direct comparison of magnetic resonance imaging and pathological shrinkage patterns of triple-negative breast cancer after neoadjuvant chemotherapy

Katsuhiro Yoshikawa
Kansai Medical University, Department of Pathology and Clinical Laboratory
Mitsuaki Ishida (ishidamt@hirakata.kmu.ac.jp)
Naoki Kan
Kansai Medical University, Department of Radiology
Hirotsugu Yanai
Kansai Medical University, Department of Surgery
Koji Tsuta
Kansai Medical University, Department of Pathology and Clinical Laboratory
Mitsugu Sekimoto
Kansai Medical University, Department of Surgery
Tomoharu Sugie
Kansai Medical University, Department of Surgery

Research

Keywords: triple-negative breast cancer, magnetic resonance imaging, neoadjuvant chemotherapy, residual tumor diameter, predictive equation.

Posted Date: April 28th, 2020

DOI: https://doi.org/10.21203/rs.3.rs-23891/v1

Version of Record: A version of this preprint was published on July 21st, 2020. See the published version at https://doi.org/10.1186/s12957-020-01959-9.

Abstract

Background We aimed to investigate the usefulness of magnetic resonance imaging (MRI) and histopathological shrinkage patterns to formulate a predictive equation for estimating residual tumor size after neoadjuvant chemotherapy (NAC) in triple-negative breast cancer (TNBC) patients.

Methods We enrolled 34 TNBC patients who underwent MRI before and after NAC. The MRI and histopathological shrinkage patterns were analyzed and classified into five categories—types I and II (concentric shrinkage without or with surrounding lesions, respectively), type III (shrinkage with residual multinodular lesions), type IV (diffuse contrast enhancement in the entire quadrant), and non-visualization. The residual tumor sizes following MRI and histopathological examination were also compared.

Results The most common MRI and histopathological shrinkage pattern was type I (41.2% and 38.2%, respectively), followed by non-visualization (26.5% and 32.4%, respectively); the concordance rate between MRI and histopathological shrinkage patterns was 41.2%. There was a strong correlation between MRI tumor size and pathological tumor size (r = 0.89). Based on these findings, a predictive equation for pathological tumor size was formulated as follows: pathological tumor size \left(mm\right) = 1.1502 \times \left(MRI tumor size \right[mm\left]\right) + 8.4277.

Conclusions Our equation may aid accurate preoperative assessment. Further studies are needed to determine its predictive value and applicability.

Background

Triple-negative breast cancer (TNBC), defined by a lack of estrogen receptor, progesterone receptor, and human epidermal growth factor receptor 2 (HER2) expression, is a high-grade phenotype of breast cancer with a poor prognosis [1, 2]. Patients with TNBC therefore often require adjuvant chemotherapy. Several large randomized clinical trials have demonstrated equivalent efficacy between neoadjuvant chemotherapy (NAC) and adjuvant chemotherapy and suggest that NAC improves the success rate of breast-conserving surgery (BCS) [3–8]. Therefore, NAC is particularly recommended for patients with TNBC who are intended to receive BCS [9]. However, because patients undergoing NAC have higher local recurrence rates, the extent of resection must be carefully determined [10].

Magnetic resonance imaging (MRI) is widely used and plays a pivotal role in guiding the extent of breast surgery by providing estimates of the tumor size and distribution after NAC [11, 12]. The superiority of MRI over ultrasound and mammography is well recognized [13]. Obtaining accurate imaging information on the extent and distribution of residual carcinoma after NAC is of utmost importance, as over-estimation of the residual tumor size may lead to unnecessary mastectomies. Conversely, under-estimation may result in tumors on ink followed by additional surgeries. Despite this, there are very few reports comparing MRI and histopathology in terms of shrinkage patterns and tumor size. Our study intended to analyze the detailed radiopathological correlation between MRI patterns before and after NAC

and pathological tumor residual patterns in patients with TNBC. The tumor diameter after NAC was also evaluated using MRI, and a predictive equation was developed to estimate the residual tumor diameter based on these findings.

Methods

Patient selection

We enrolled 165 consecutive patients with TNBC who underwent surgical resection at the Department of Surgery of the Kansai Medical University Hospital between January 2006 and December 2018. Patients who did not receive NAC or did not undergo MRI before and after NAC were excluded from the study; finally, 34 patients with TNBC were included.

This study was conducted in accordance with the principles of the Declaration of Helsinki, and the study protocol was approved by the Institutional Review Board of the Kansai Medical University Hospital (protocol no.: 2019041). Informed consent was individually obtained from all participants included in the study

Chemotherapy

The NAC regimens were selected based on patients' preferences. Overall, 33 (97%) patients received sequential anthracycline- and taxane-based regimens. The anthracycline-based regimens included EC (epirubicin: 100 mg/m^2 and cyclophosphamide: 500 mg/m^2), AC (doxorubicin: 60 mg/m^2 and cyclophosphamide: 600 mg/m^2), and FEC (epirubicin: 100 mg/m^2, cyclophosphamide: 500 mg/m^2, and 5-fluorouracil: 500 mg/m^2). Chemotherapy was administered every 3 weeks for 4 cycles. The taxane-based regimens included docetaxel at a dose of 70 mg/m^2 every 3 weeks for 4 cycles, or weekly paclitaxel at a dose of 80 mg/m^2 for 12 doses with scheduled rests. Only one patient received a taxane-based regimen without anthracyclines (docetaxel 75 mg/m^2 and cyclophosphamide 600 mg/m^2).

MRI technique

MRI was performed using 1.5-T scanners (Signa Excite HD; GE Healthcare, Milwaukee, WI, USA) with a dedicated breast coil. All images were obtained in the prone position. All patients received intravenous contrast (0.1 mmol/kg gadopentetate dimeglumine).

MRI was performed 2 to 4 weeks prior to, and following completion of NAC.

Interpretation of MRI

Two experienced breast surgeons and one experienced breast-imaging radiologist conjointly reviewed the pre- and post-NAC breast MRI findings of all patients.

The contrast-enhanced MRI patterns prior to NAC were classified into five categories, as described by Tomida et al. [14]—solitary, grouped (localized lesion with linear and/or spotty enhancement), separated

(multiple foci of contrast enhancement), mixed (grouped lesion with multiple foci), and replaced (diffuse contrast enhancement in entire quadrant) lesions. The MRI shrinkage patterns of breast cancer following NAC were classified into five categories, as suggested by Kim et al. [15]—type I (concentric shrinkage without any surrounding lesion), type II (concentric shrinkage with surrounding lesions), type III (shrinkage with residual multi- nodular lesions), type IV (diffuse contrast enhancement in entire quadrant), and non-visualization. Breast cancer reactions after NAC were determined using the response evaluation criteria in solid tumors classification [16], based on unidimensional measurements of the largest tumor diameter.

Histopathological examination

The histopathological diagnosis of the breast cancers was independently performed by two experienced diagnostic pathologists. The response following NAC was assessed based on the Miller–Payne grading system, established by Ogston et al. [17]. The grades are as follows: grade 1, no change or particular alteration to individual malignant cells and no reduction in overall cellularity; grade 2, minor loss of tumor cells (≤ 30%) with overall cellularity remaining high; grade 3, an estimated 30 to 90% reduction in tumor cells; grade 4, a marked disappearance of tumor cells so that only small clusters or widely dispersed individual cells remain, with > 90% loss of tumor cells; and grade 5, no malignant cells identified in sections from the tumor site, only vascular fibroelastic stroma remaining, often containing macrophages, with possible presence of intraductal carcinoma components.

The histopathological patterns of the residual tumor were also classified into five categories, similar to the classification of MRI shrinkage patterns [14]. Histopathological tumor size was determined based on unidimensional measurements of the largest tumor diameter (including ductal component). A free margin of 2 mm or less was defined as positive [18].

Statistical Analysis

All analyses were performed using SPSS Statistics 25.0 software (IBM, Armonk, NY. USA). Agreement between two groups was analyzed using the Kappa test.

The Pearson's correlation coefficient was used to compare tumor size on MRI with the histological tumor size. A P value of less than 0.05 was regarded as significant.

Results

Patients' characteristics

The characteristics of patients in the present cohort are summarized in Table 1. This study included 34 patients; all were female. The median age at the time of initial diagnosis was 53 (range: 31–77) years. All patients were diagnosed with TNBC based on the biopsy specimens; 31, 2, and 1 patients were diagnosed with invasive carcinoma of no special type, apocrine carcinoma, and invasive lobular carcinoma, respectively. Ten patients were initially diagnosed with clinical stage I, 10 with stage IIA, 9 with stage IIB, 2 with stage IIIA, 1 with stage IIIB, and 2 with stage IIIC.

Table 1
Clinical characteristics of patients with triple negative breast cancer

Factor		Median (range)	n	%
Total			34	
Age (years)		53 (31–77)		
Menopausal status				
	Premenopausal		11	32.4
	Postmenopausal		20	58.8
	Unknown		3	8.8
Histology				
	Invasive carcinoma, no special type		31	91.2
	Invasive lobular carcinoma		1	2.9
	Apocrine carcinoma		2	5.9
Initial clinical stage				
			10	29.4
	A		10	29.4
	B		9	26.5
	A		2	5.9
	B		1	2.9
	C		2	5.9
Ki-67				
	Low (≤ 20%)		2	5.9
	High (> 20%)		29	85.3
	Unknown		3	8.8
Lymph node metastasis				
	Present		15	44.1
	Absent		19	55.9
Neoadjuvant chemotherapy regimen				
	Taxane		1	2.9

Factor		Median (range)	n	%
	Taxane + ant		33	97.1
Type of surgery				
	Radical mastectomy		11	32.4
	Partial mastectomy		23	67.6

MRI findings before and after NAC

The most common enhancement pattern before NAC was solitary (20 patients, 58.8%), followed in order by separated (7 patients, 20.6%), grouped (5 patients, 14.7%), and replaced (2 patients, 5.9%) lesions (Fig. 1a–d; Table 2). None of the patients in the present study showed mixed enhancement patterns.

Table 2 summarizes the tumor shrinkage patterns after NAC. The most common shrinkage pattern on MRI was type I (14 patients, 41.2%), followed in order by non-visualization (9 patients, 26.5%), type III (5 patients, 14.7%), type II (4 patients, 11.8%), and type IV (2 patients, 5.9%). For the association between the initial findings and shrinkage patterns in MRI, the most common shrinkage pattern (type I) was observed in 60% of the patients with solitary patterns, followed by non-visualization, which was observed in 30% (Table 2). Patients with non-visualization patterns after NAC initially had either solitary or separated enhancement patterns.

Table 2
Correlation between initial contrast-enhancement patterns prior to neoadjuvant chemotherapy and shrinkage patterns

	Initial enhancement patterns			
Shrinkage patterns	Solitary	Grouped	Separated	Replaced
Non-visualization	6	0	3	0
Type	12	1	1	0
Type	1	2	1	0
Type	1	2	2	0
Type	0	0	0	2

Histopathological features following NAC

The most common histopathological regression grade was 1 (12 patients, 35.3%), followed by grades 5 (11 patients, 32.4%), 2 (6 patients, 17.6%), 4 (4 patients, 11.8%), and 3 (1 patient, 2.9%). The most common shrinkage pattern on histopathology was type I, observed in 38.2% of the patients, followed in order by non-visualization (32.1%), type III (20.6%), type II (5.9%), and type IV (2.9%) (Table 3). The observed concordance between the shrinkage patterns on MRI and on histopathology was 41.2% (Kappa

statistics: 0.181, *p = 0.07*). Subsequently, we performed a direct comparison between MRI-based and histopathological shrinkage patterns in TNBC. Among 11 patients with no residual disease, six were diagnosed as having non-visualization pattern on MRI (sensitivity, 54.5%). In the other five patients, type I MRI shrinkage pattern was observed in 1 patient, type II in 2, and type III in 2 other patients (Table 3). Among the 23 patients who had residual disease, three did not show contrast-enhanced lesions on MRI (specificity 87.0%)

Table 3
Correlation between MRI shrinkage patterns and pathological shrinkage patterns following neoadjuvant chemotherapy

	Pathological shrinkage pattern				
	Non-visualization	Type □	Type □	Type □	Type □
MRI shrinkage pattern					
Non-visualization	6	2	0	1	0
Type □	1	8	1	3	1
Type □	2	0	0	2	0
Type □	2	2	1	0	0
Type □	0	1	0	1	0

Relationship between MRI and histopathological tumor sizes after NAC

Next, we assessed the residual tumor size on MRI and on histopathology after NAC in 25 patients with TNBC. There was a significant correlation between MRI tumor size and histopathological tumor size (Pearson's correlation coefficient of 0.89, $p < 0.0001$). The mean difference between MRI-based and histopathology-based tumor diameter was 11.5 ± 12.7 mm. The following equation was developed based on the findings:

$$Pathological residual tumor size\,(mm) = 1.1502 \times (residual tumor size[\,mm\,]) + 8.4277$$

If a resection size was estimated based on this equation before surgery, a safe margin of 10 mm beyond the calculated pathological size would lead to a positive margin rate of 4%. Moreover, a 20-mm safe margin would result in a positive margin rate of 0%.

Discussion

In the present study, we demonstrated a significant correlation between MRI and histopathology for residual tumor size and obtained a predictive equation to estimate the size of residual tumors using MRI

results. Furthermore, the correlation between MRI and histopathological shrinkage patterns in patients with TNBC after NAC was relatively high.

Several reports have elucidated the shrinkage patterns of breast cancer after NAC. Kim et al. studied the shrinkage tumor patterns on MRI following NAC, and they reported that the most common MRI shrinkage patterns in breast cancer patients were type I (51.8%), followed by type II (23.2%) [15]. Tomida et al. studied the correlation between MRI shrinkage patterns and pathological shrinkage patterns following NAC. They reported that the most common pathological shrinkage pattern was type II (40.7%), followed by type III (29.6%), and the concordance rate between MRI and histopathological patterns was 48% [14]. However, these two studies did not examine the relationship between the shrinkage patterns of various molecular subtypes of breast cancer. In the present study, the high rate of type (41.2%), the relatively high rate of non-visualization (26.5%), and the low rate of type II (11.8%) patterns may be a characteristic feature of MRI shrinkage patterns in TNBC. Furthermore, the present study found that high frequencies of type I (38.2%) and non-visualization (32.4%) pathological shrinkage patterns were characteristic of TNBC. The concordance rate of 41.2% between MRI and pathological shrinkage patterns in the present cohort was comparable to that of the previous report (48%), in which no distinction among molecular subtypes was found [14].

Because of the high effectiveness of chemotherapy observed in patients with TNBC [19], our study resulted in a high frequency of the “non-visualization” pathological pattern, compared to previous reports [14, 15]. Moreover, the high frequency of type pathological shrinkage pattern suggests that the concentric shrinkage pattern may be more commonly found in TNBC than in other molecular subtypes after NAC. These characteristics of TNBC may be attributed to differences in the efficacy of NAC, evidenced by the variation observed in the tumor shrinkage patterns after NAC among different molecular subtypes.

MRI is known to be useful for predicting pathological complete responses (pCR) after NAC. Liu et al. reported a high specificity (88%) and relatively low sensitivity (65%) for MRI in predicting pCR among patients with breast cancer [20]. Although the molecular subtypes were not classified in their reports, the results of the present study concur with theirs. Therefore, TNBC may have a similar tendency to other molecular subtypes on pCR prediction.

Nakahara et al. reported that TNBC showed a significant correlation between the residual tumor sizes obtained on MRI and pathological tumor sizes after NAC [21]. However, an MRI-based predictive equation for residual tumor size has yet to be developed. The development of an accurate MRI-based measurement tool is of particular necessity for patients receiving NAC and BCS, a matter that needs to be urgently addressed. Our predictive equation may help to estimate accurately tumor size and to reduce the high rate (2–40%) of tumors on ink reported in patients undergoing BCS after NAC [22].

The present study had several limitations. First, it was a retrospective single-institution study with a small sample size, and therefore, selection bias was a possibility. Second, the present study only analyzed TNBC. Since the MRI and pathological shrinkage patterns after NAC may be influenced by molecular

subtypes, further studies are needed to investigate the characteristics of residual carcinoma after NAC in patients with various molecular types of breast cancer. Third, for our predictive equation, a validation study is required before it can be formally used; therefore, additional studies are needed to evaluate its applicability.

Conclusions

In the present study, we investigated the characteristics of MRI and pathological shrinkage patterns and their relationship in patients with TNBC. We also developed a useful equation for estimating the size of residual cancer after NAC in patients with TNBC, based on the size noted on MRI. The newly developed equation may improve the success rates for BCS after NAC among patients with TNBC.

List Of Abbreviations

BCS - breast-conserving surgery

HER2 - human epidermal growth factor receptor 2

MRI - magnetic resonance imaging

NAC - neoadjuvant chemotherapy

pCR - pathological complete responses

TNBC - triple-negative breast cancer

Declarations

Ethics approval and consent to participate

All procedures performed in studies involving human participants were completed in accordance with the ethical standards of the institutional and/or national research committee and with the 1964 declaration of Helsinki and its later amendments or comparable ethical standards.

Informed consent: Informed consent was obtained from all individual participants included in the study.

Consent for publication

Not applicable.

Availability of data and materials

The datasets used and/or analyzed during the current study are available from the corresponding author on reasonable request.

Competing interests

The authors declare no conflict of interest.

Funding

This research did not receive any specific grant from funding agencies in the public, commercial, or not-for-profit sectors.

Authors' contributions

KY analyzed and interpreted the patient data regarding the triple negative breast cancer after neoadjuvant chemotherapy. MI and KY performed the histological examination of the breast and were major contributors in the writing of the manuscript. NK and KY reviewed the MRI findings. HY, KT, MS and TS contributed to data interpretation. All authors read and approved the final manuscript.

Acknowledgements

Not applicable

Authors' information

Affiliations

Department of Pathology and Clinical Laboratory, Kansai Medical University, 2-5-1, Shinmachi, Hirakata City, Osaka, Prefecture, Japan

Katsuhiro Yoshikawa, Mitsuaki Ishida, Koji Tsuta

Department of Surgery, Kansai Medical University, 2-5-1, Shinmachi, Hirakata City, Osaka, Prefecture, Japan

Katsuhiro Yoshikawa, Hirotsugu Yanai, Mitsugu Sekimoto, Tomoharu Sugie

Department of Radiology, Kansai Medical University, 2-5-1, Shinmachi, Hirakata City, Osaka, Prefecture, Japan

Naoki Kan

Corresponding author

Correspondence to Mitsuaki Ishidsa

References

1. Cleator S, Heller W, Coombes RC. Triple-negative breast cancer: therapeutic options. Lancet Oncol. 2007;8:235–44.
2. Dent R, Trudeau M, Pritchard KI, Hanna WM, Kahn HK, Sawka CA, et al. Triple-negative breast cancer: clinical features and patterns of recurrence. Clin Cancer Res. 2007;13:4429–34.
3. Fisher B, Brown A, Mamounas E, Wieand S, Robidoux A, Margolese RG, et al. Effect of preoperative chemotherapy on local-regional disease in women with operable breast cancer: findings from National Surgical Adjuvant Breast and Bowel Project B-18. J Clin Oncol. 1997;15:2483–93.
4. Fisher B, Bryant J, Wolmark N, Mamounas E, Brown A, Fisher ER, et al. Effect of preoperative chemotherapy on the outcome of women with operable breast cancer. J Clin Oncol. 1998;16:2672–85.
5. Mamounas EP, Fisher B. Preoperative (neoadjuvant) chemotherapy in patients with breast cancer. Semin Oncol. 2001;28:389–99.
6. Goldhirsch A, Glick JH, Gelber RD, Coates AS, Senn HJ. Meeting highlights: International Consensus Panel on the Treatment of Primary Breast Cancer. Seventh International Conference on Adjuvant Therapy of Primary Breast Cancer. J Clin Oncol. 2001;19:3817–27.
7. Mauri D, Pavlidis N, Ioannidis JP. Neoadjuvant versus adjuvant systemic treatment in breast cancer: a meta-analysis. J Natl Cancer Inst. 2005;97:188–94.
8. Mieog JS, van der Hage JA, van de Velde CJ. Preoperative chemotherapy for women with operable breast cancer. Cochrane Database Syst Rev. 2007;2:CD005002.
9. Golshan M, Cirrincione CT, Sikov WM, Berry DA, Jasinski S, Weisberg TF, et al. Impact of neoadjuvant chemotherapy in stage II-III triple negative breast cancer on eligibility for breast-conserving surgery and breast conservation rates: surgical results from CALGB 40603 (Alliance). Ann Surg. 2015;262:434–9.
10. Akay CL, Meric-Bernstam F, Hunt KK, Grubbs EG, Bedrosian I, Tucker SL, et al. Evaluation of the MD Anderson Prognostic Index for local-regional recurrence after breast conserving therapy in patients receiving neoadjuvant chemotherapy. Ann Surg Oncol. 2012;19:901–7.
11. Marinovich ML, Houssami N, Macaskill P, Sardanelli F, Irwig L, Mamounas EP, et al. Meta-analysis of magnetic resonance imaging in detecting residual breast cancer after neoadjuvant therapy. J Natl Cancer Inst. 2013;105:321–33.
12. Chen JH, Bahri S, Mehta RS, Carpenter PM, McLaren CE, Chen WP, et al. Impact of factors affecting the residual tumor size diagnosed by MRI following neoadjuvant chemotherapy in comparison to pathology. J Surg Oncol. 2014;109:158–67.
13. Marinovich ML, Macaskill P, Irwig L, Sardanelli F, Mamounas E, von Minckwitz G, et al. Agreement between MRI and pathologic breast tumor size after neoadjuvant chemotherapy, and comparison with alternative tests: individual patient data meta-analysis. BMC Cancer. 2015;15:662.
14. Tomida K, Ishida M, Umeda T, Sakai S, Kawai Y, Mori T, et al. Magnetic resonance imaging shrinkage patterns following neoadjuvant chemotherapy for breast carcinomas with an emphasis on the radiopathological correlations. Mol Clin Oncol. 2014;2:783–8.

15. Kim TH, Kang DK, Yim H, Jung YS, Kim KS, Kang SY. Magnetic resonance imaging patterns of tumor regression after neoadjuvant chemotherapy in breast cancer patients: correlation with pathological response grading system based on tumor cellularity. J Comput Assist Tomogr. 2012;36:200–6.
16. Therasse P, Arbuck SG, Eisenhauer EA, Wanders J, Kaplan RS, Rubinstein L, et al. New guidelines to evaluate the response to treatment in solid tumors. European Organization for Research and Treatment of Cancer, National Cancer Institute of the United States, National Cancer Institute of Canada. J Natl Cancer Inst. 2000;92:205–16.
17. Ogston KN, Miller ID, Payne S, Hutcheon AW, Sarkar TK, Smith I, et al. A new histological grading system to assess response of breast cancers to primary chemo- therapy: prognostic significance and survival. Breast. 2003;12:320–7.
18. Marinovich ML, Azizi L, Macaskill P, Irwig L, Morrow M, Solin LJ, et al. The association of surgical margins and local recurrence in women with ductal carcinoma in situ treated with breast - conserving therapy: a meta - analysis. Ann Surg Oncol. 2016;23:3811–21.
19. Wu K, Yang Q, Liu Y, Wu A, Yang Z. Meta-analysis on the association between pathologic complete response and triple-negative breast cancer after neoadjuvant chemotherapy. World J Surg Oncol. 2014;12:95.
20. Liu Q, Wang C, Li P. The role of (18)F-FDG PET/CT and MRI in assessing pathological complete response to neoadjuvant chemotherapy in patients with breast cancer: A systematic review and meta-analysis. Biomed Res Int. 2016;2016:3746232.
21. Nakahara H, Yasuda Y, Machida E, Maeda Y, Furusawa H, Komaki K, et al. MR and US imaging for breast cancer patients who underwent conservation surgery after neoadjuvant chemotherapy: comparisonof triple negative breast cancer and other intrinsic subtypes. Breast Cancer. 2011;18:152–60.
22. Volders JH, Negenborn VL, Spronk PE, Krekel NMA, Schoonmade LJ, Meijer S, et al. Breast-conserving surgery following neoadjuvant therapy-a systematic review on surgical outcomes. Breast Cancer Res Treat. 2018;168:1–12.

Figures

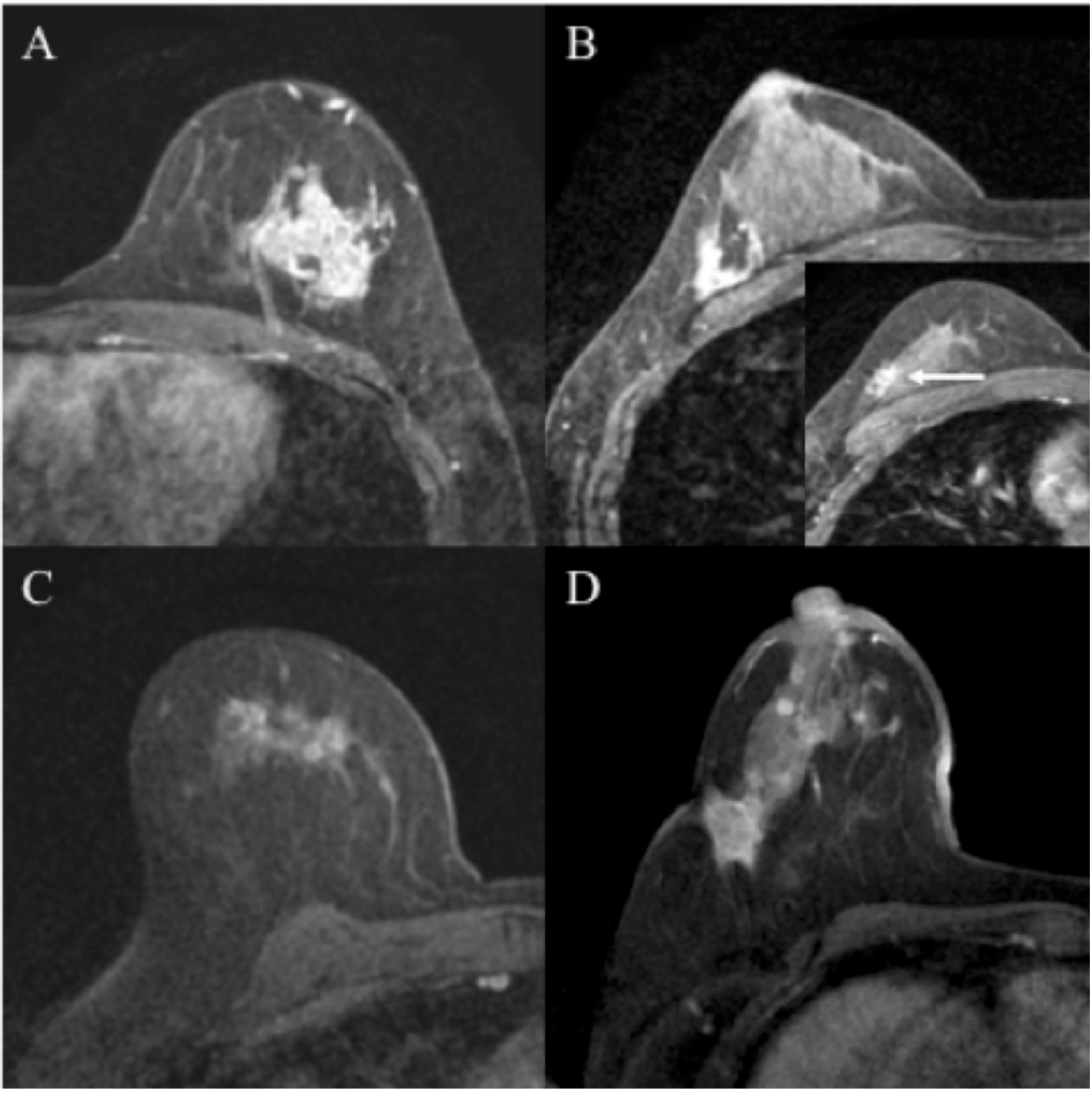

Figure 1

Magnetic resonance images of the initial enhancement patterns of triple-negative breast cancer prior to neoadjuvant chemotherapy. (A) Solitary, (B) Separated (arrow shows the daughter nodule), (C) Grouped, and (D) Replaced

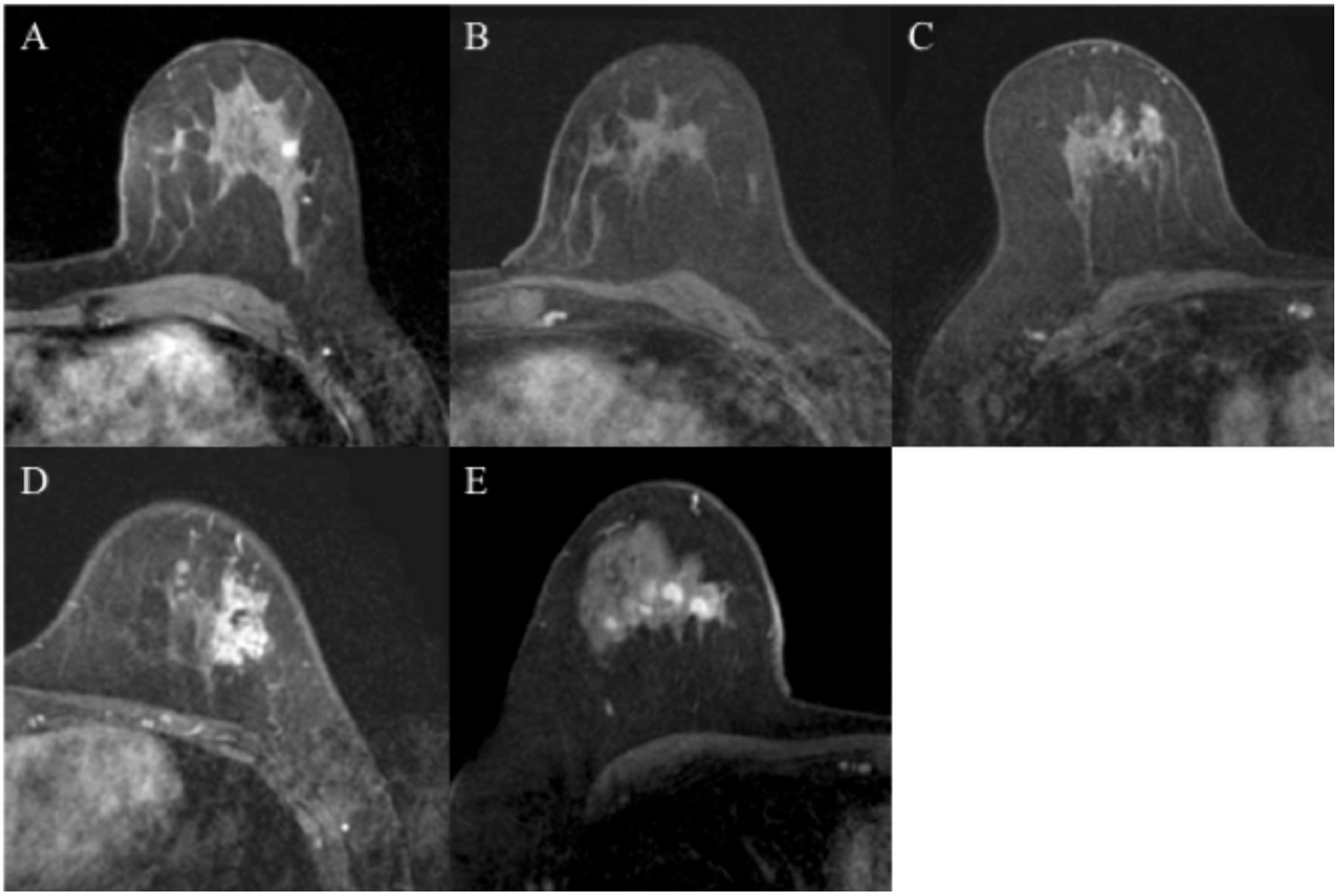

Figure 2

Magnetic resonance images of the shrinkage patterns of triple-negative breast cancer following neoadjuvant chemotherapy. (A) Concentric shrinkage without any surrounding lesions, type I; (B) non-visualization; (C) Residual multinodular lesions, type III; (D) Concentric shrinkage pattern with surrounding lesions, type II; (E) Diffuse contrast enhancement in entire quadrant, type IV

Figure 3

Panoramic view of the histopathological shrinkage patterns and features following neoadjuvant chemotherapy. (A) Pathological type I showing concentric shrinkage without any surrounding lesions. (B) Pathological type III demonstrating shrinkage with residual multinodular lesions. (C) Pathological type II showing concentric shrinkage with surrounding lesions. (D) Pathological type IV demonstrating multiple residual carcinomas (arrows: residual carcinoma cells); hematoxylin and eosin staining

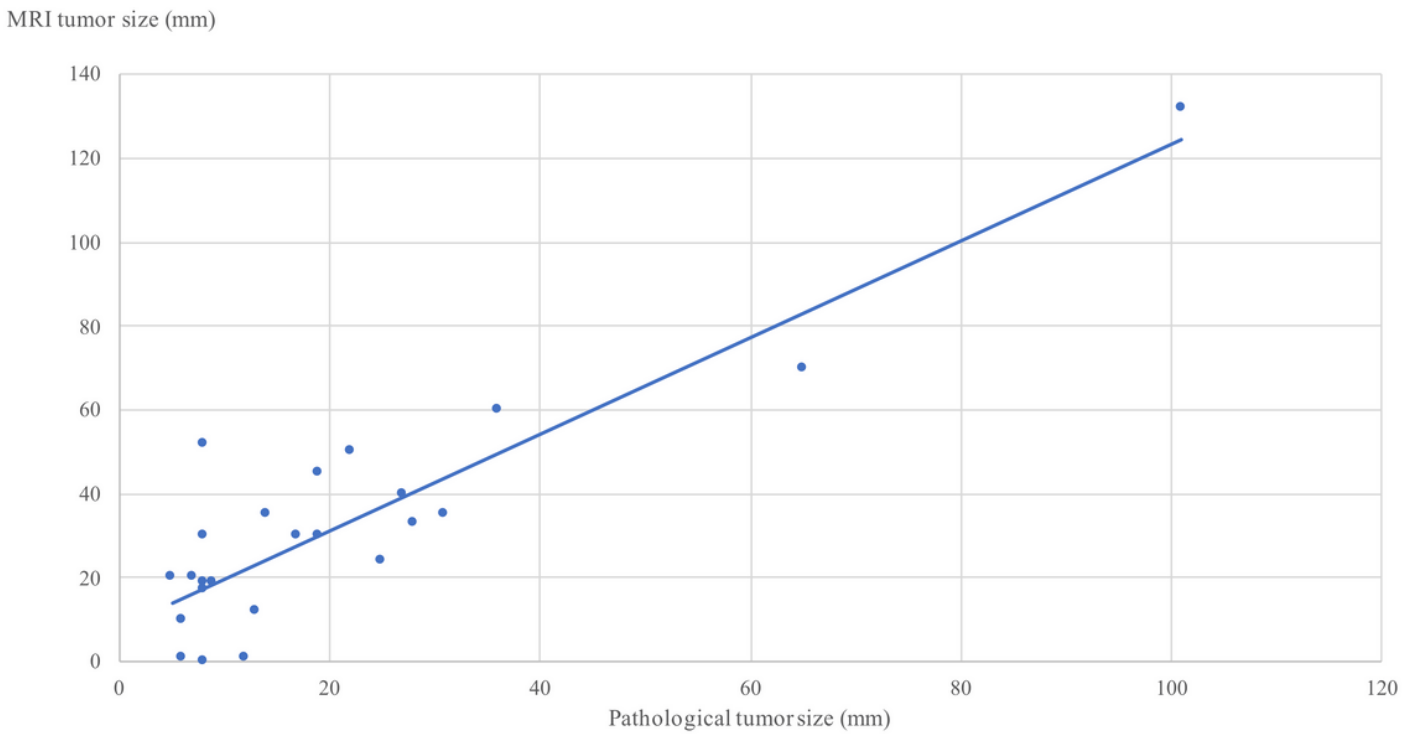

Figure 4

Correlation between MRI and pathological tumor sizes in patients with non-clinical complete remission. Correlation coefficient (r) = 0.89 (p <0.0001)